NASA TECHNICAL TRANSLATION NASA TT F-16172

EFFECT OF TITANIUM, BORON AND MOLYBDENUM ON THE STRUCTURE OF AUSTENITIC 18/10 STEEL AFTER SOLUTION HEAT TREATMENT AND SENSITIZATION

Z. Bojarski, W. Czyrski,
J. Eysymontt and H. Serwicki

Institute of Ferrous Metallurgy

Translation of "Wplyw tytanu, boru i molibdenu na strukture stali austenitycznych 18/10 w stanie przesyconym i po wyzarzaniu uczulajacym," Prace Instytutow Hutniczych, vol. 23, no. 1, 1971, pp. 9-23.

NATIONAL AERONAUTICS AND SPACE ADMINISTRATION
WASHINGTON, D.C. 20546 MARCH 1975

STANDARD TITLE PAGE

1. Report No.	2. Government Accession No.	3. Recipient's Catalog No.
TT F-16172		

4. Title and Subtitle	5. Report Date
EFFECT OF TITANIUM, BORON AND MOLYBDENUM ON THE STRUCTURE OF AUSTENITIC 18/10 STEEL AFTER SOLUTION HEAT TREATMENT AND SENSITIZATION	March 3, 1975
	6. Performing Organization Code

7. Author(s)	8. Performing Organization Report No.
Z. Bojarski et al. Institute of Ferrous Metallurgy	10. Work Unit No.

9. Performing Organization Name and Address	11. Contract or Grant No.
Leo Kanner Associates Redwood City, CA 94063	NASw 2481
	13. Type of Report and Period Covered
	Translation
12. Sponsoring Agency Name and Address	14. Sponsoring Agency Code
National Aeronautics and Space Administration, Washington, D.C. 20546	

15. Supplementary Notes

Translation of "Wplyw tytanu, boru i molibdenu na strukture stali austenitycznych 18/10 w stanie przesyconym i po wyzarzaniu uczulajacym," Prace Instytutow Hutniczych, vol. 23, no. 1, 1971, pp. 9-23.

16. Abstract

Austenitic steels types OH18N9, IH18N10T, IH18N10T+B and IH18N10MT manufactured in Poland and imported X10CrNiTi X10CrNiTi18·9 steel were investigated after solution heat treatment and annealing at 500, 650 and 750°C. The methods used were optical and electron microscopy, x-ray phase analysis and x-ray microanalysis. The following inclusions were observed in solution heat treated steels: in OH18N9 steel nonmetallic oxide and sulfide inclusions and in the remaining types of steels also carbide, titanium nitride and $Ti_4S_2C_2$ inclusions. After the sensitizing treatment the $M_{23}C_6$ carbide was precipitated in OH18N9 steel, the $M_{23}C_6$ carbide and small amounts of the S phase in OH18N16T, IH18N10MT and IH18N10T+B steel, the σ phase and a small amount of $M_{23}C_6$ carbide in IH18N10MT steel and only a small amount of the σ phase in X10CrNiTi18·9 steel. There is no conclusive evidence demonstrating the effect of boron on the precipitation process.

17. Key Words (Selected by Author(s))	18. Distribution Statement
	UNCLASSIFIED-UNLIMITED

19. Security Classif. (of this report)	20. Security Classif. (of this page)	21. No. of Pages	22. Price
Unclassified	Unclassified	32	

EFFECT OF TITANIUM, BORON AND MOLYBDENUM ON THE STRUCTURE OF AUSTENITIC 18/10 STEEL AFTER SOLUTION HEAT TREATMENT AND SENSITIZATION

Z. Bojarski, W. Czyrski,
J. Eysymontt and H. Serwicki

Institute of Ferrous Metallurgy

1. Introduction

The manufacture of high quality acid resisting steels is becoming particularly important in conjunction with the development of the chemical industry. The useful properties of these steels depend on their structure, which in turn is influenced by the chemical composition, the smelting technology, their plasticity and the heat treatment. This study is a part of more extensive studies carried out in the Institute of Ferrous Metallurgy. It investigates the effect of changes in the chemical composition and in the so-called sensitizing annealing parameters on the structure of austenitic acid resisting steels. 79

2. Materials Studied

The following domestic industrial steel melts were used in the studies: (OH18N0 (melt 58374), IH18N1oT (melt 58731), IH18N10-T+B (melt 58802), IH18N10MT (melt 58731), IH18N10T (melt 69240) and imported material manufactured by Avesta Jernverks Aktienbolag, grade X10CrNiTi189 (IH18N10T"s").

The domestic material was received partially in the form of 15 mm diameter rods and partially in the form of rods with a 27 mm square cross-section, which were subsequently reforged to a 20 mm diameter cross section. The imported steel was received in the form of 20 mm thick sheets. On the average the dimensions of the

*Numbers in the margin indicate pagination in the foreign text.

rolled specimens were 15 mm (diameter) x 45 mm (length). The chemical composition of the steels studied is given in Table 1.

All steels were subjected to solution heat treatment in water for 30 minutes at 1050°C. Subsequently the specimens were annealed according to the following variants:

a. 500°C: 10, 50, 100 and 3000 hours
b. 650°C: 15 min, 1, 5, 10, 100 and 1000 hours
c. 750°C: 5 min, 1, 5, 10, 100 and 1000 hours and cooled in air.

All specimens were examined under a light microscope, whereas for the studies using an electron microscope and for the x-ray studies, we selected specimens which were annealed for 10, 100 and 1000 hours at each of the three temperatures given above.

3. Method Used in Studies

To obtain the necessary information on the structure of the steels studied in relation to the heat treatment conditions, we used the following research methods:

a. Studies of the structure of cast specimens, using the Neophot light microscope manufactured by the firm Zeiss (GDR) whose purpose was to identify nonmetallic inclusions and to obtain preliminary information on the character of the matrix and relatively large precipitates.

b. Studies, using the JXA-3A x-ray microanalyzer manufactured by the firm JEOL (Japan), whose purpose was to determine the chemical composition of the nonmetallic inclusions and large precipitates by means of known methods [1].

c. Indirect studies (using the method of replicas) and direct studies (using the method of thin foils) of the structure of cast specimens and extracted precipitates using the JEM-7 electron microscope manufactured by the firm JEOL (Japan). The replicas were made using generally known methods [2], [3], and the thin foils were

obtained by the Bollmann method [3], [4], [5], [6]. The objective of the studies was to determine the size and shape of the precipitates and to make the identification using the electron diffraction method on the basis of the microscope constant calculated from a gold sample sputtered on a part of the replicas. In the case of thin foils the austenite was treated as an internal standard.

d. Determination of the amount of segregations and x-ray metallography studies of the phase composition of segregations to determine the properties of the precipitation process and the type of precipitates. The precipitates were separated electrolytically in a 10% HCl solution in ethanol at a 0.02 A/cm^2 current density. The percentage segregation content was calculated from the segregation mass and the mass decrement in the sample. The phase composition of the segregation was determined from x-ray photographs made using a 114.6 mm circular camera and KaCo rays.

e. Hardness measurements using the hardness meter manufactured by the firm Vickers (England) under a 30 kg load.

Other methods were also used to complete the studies, for example detection of the phases by interference layer sputtering.

4. Results of the Studies

4.1. OH18N9 Steel

4.1.1. Original structure (after solution heat treatment)

The light microscope studies of unetched metallographic specimens showed the presence of sulfides and oxides. This was confirmed by the x-ray microanalyzer studies. The light microscope studies of etched metallographic specimens revealed a pure austenitic structure (without δ-Fe) with a small amount of regularly shaped precipitates. The electron microscope studies detected an austenitic structure with weakly marked grain boundaries. Few relatively large precipitates were detected on the grain boundary. According to the x-ray phase analysis the segregations included traces of vanadium carbide (0.27 weight % VC). The hardness of the steel was HV = 144.

4.1.2. Structure after annealing

Light microscope studies of annealed specimens did not reveal any structural changes at 500°C in comparison with heat solution treatment. Annealing at 650°C causes much more pronounced etching /12 of grain boundaries than solution heat treatment. Especially large precipitates were visible on the grain boundaries after a long annealing time. Specimens annealed at 750°C have precipitates along the grain boundaries whose size increases with the annealing time and precipitates in grains which are clearly visible after an annealing time exceeding 100 hours.

Electron microscope studies of specimens annealed at 500°C for 10, 100 and 1000 hours did not reveal the precipitation process. The precipitation of very small carbides (Fig. 1) along the grain boundaries was only detected in an additional test specimen annealed for 3000 hours. Several groups of minute precipitates, not always bounded by grain boundaries were detected in a specimen annealed at 650°C for 10 hours. Only annealing for 100 hours at the same temperature caused clearly visible precipitation of carbides (Fig. 2) identified on the semiextraction replicas by selective electron diffraction as $M_{23}C_6$ (Fig. 3). The use of extraction replicas made it possible to detect a very large number of carbides along the grain boundaries (Fig. 4). It was established that the preferred location for the precipitation of $M_{23}C_6$ carbides are not only the grain boundaries, but also the zones around large inclusions or primary precipitates (Fig. 5). $M_{23}C_6$ carbides were detected in a specimen annealed at 650°C for 1000 hours both on the grain boundaries and in the grains. Very large carbides occur along the grain boundaries. These probably originated as a result of the increase in many smaller carbides precipitated earlier, as well as minute carbides, which also occur in the grains (Fig. 6). A strip-like growth of carbides into the depth of one grain (Fig. 7) or two grains (Fig. 8) can be seen in some spots on the grain boundaries. This kind of carbide growth was observed also in the center of the grain and it begins on a large primary precipitate (Figs. 9, 10). The

carbides represented in Fig. 10 were identified by electron diffraction as $M_{23}C_6$. Triangular shaped carbide growth zones (Fig. 11) were observed in many grains. These were also identified as $M_{23}C_6$. The $M_{23}C_6$ carbides which occur along the grain boundaries in specimens annealed at 750°C have larger dimensions than before. They have irregular shapes with rounded corners (Fig. 12). On the other hand, large triangular fields, primarily grown carbides, occur in the grains (Fig. 13). Studies of the amount of segregations (Fig. 14) did not reveal the presence of the precipitation process during annealing at 500°C. On the other hand, annealing at 650°C and 750°C causes a large increase in the amount of segregations with the annealing time.

Table 1. Chemical Composition of Steels Studied

a Stal	b Wykonawca analizy	c Zawartość pierwiastków, % C	Mn	Si	P	S	Cr	Ni	Ti	Mo	B	Nb	V	Ta	Zr
OH18N9	huta d	0,051	1,48	0,37	0,020	0,010	18,20	10,02	nb	0,14	nb	nb	nb	nb	nb
	IMŻ e	0,050	1,50	0,35	0,021	0,010	18,15	10,25	0,01	0,15	0,0026	<0,01	0,07	<0,01	0,001
1H18N 10T	huta	0,082	1,64	0,62	0,034	0,016	17,05	10,49	0,41	0,20	nb	nb	nb	nb	nb
	IMŻ	0,077	1,58	0,36	0,022	0,010	16,83	10,90	0,46	0,15	ślady	<0,01	0,07	<0,01	0,002
1H18N 10T+B	huta	0,070	1,44	0,47	0,027	0,014	17,45	10,56	0,38	nb *	0,0038	nb	nb	nb	nb
	IMŻ	0,058	1,46	0,40	0,023	0,015	17,10	10,88	0,40	0,20	0,0050	<0,01	0,07	<0,01	0,001
1H18N 10MT	huta	0,078	1,49	0,36	0,035	0,012	17,70	10,27	0,56	1,83	nb	nb	nb	nb	nb
	IMŻ	0,068	1,58	0,38	0,027	0,018	17,38	10,12	0,58	1,84	0,0035	<0,01	0,07	<0,01	0,001
1H18N 10T„s"	Avesta	0,048	1,64	0,41	0,029	0,008	17,4	10,6	0,54	0,22	nb	nb	nb	nb	nb
	IMŻ	0,07	1,67	0,40	0,020	0,009	17,85	10,64	0,52	nb	0,0015	<0,01	0,08	<0,01	0,003

Objaśnienia: nb — nie badano

f

Key: a--steel
b--analysis made by
c--element content, %
d--mill
e--Inst. of Nonferrous Metallurgy
f--remark: nb = not studied

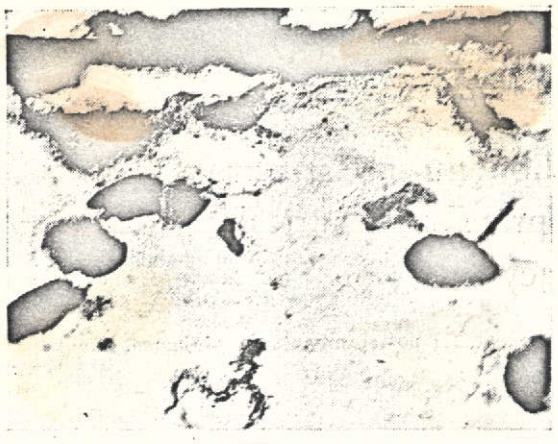

Fig. 1. OH18N9 steel. Structure after annealing for 3000 hours at 500°C. Minute $M_{23}C_6$ carbides on the boundary between grains. Electron microscope. Carbide extraction replica. Magnified 100000 x.

Fig. 2. OH18N9 steel. Structure after annealing: 650°C, 100 hours. Partially extracted $M_{23}C_6$ carbides on boundary between grains. Electron microscope. Semiextraction replica. Magnified 25000 x.

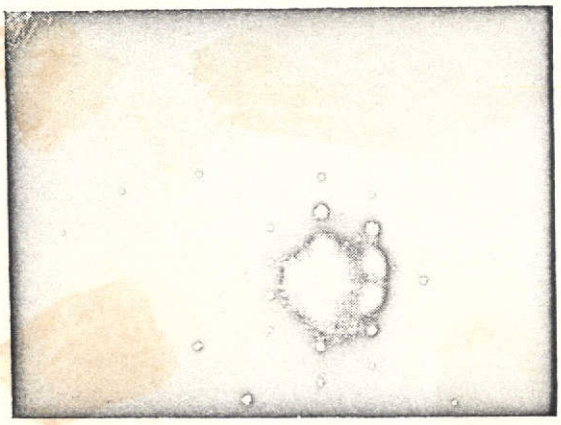

Fig. 3. OH18N9 steel. Electron diffraction pattern of single $M_{23}C_6$ carbide. Direction of incident beam [343].

Fig. 4. OH18N9 steel. Structure after annealing: 650°C, 100 hours. $M_{23}C_6$ carbides on boundary between grains. Electron microscope. Carbon extraction replica. Magnified 25000 x.

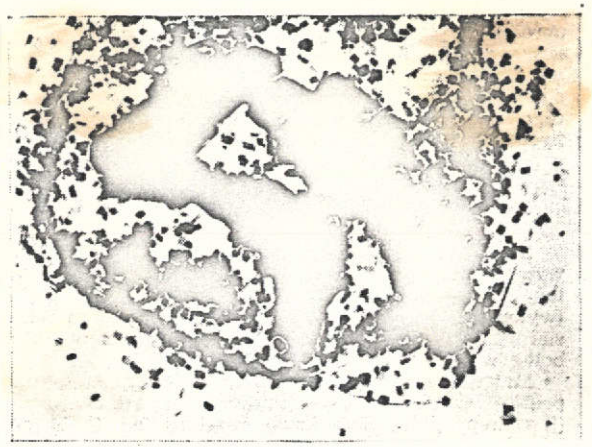

Fig. 5. OH18N9 steel. Structure after annealing: 650°C, 100 hours. Large inclusions or primary precipitates surrounded by minute precipitates are clearly visible. Electron microscope. Carbon extraction replica. Magnified 15500x.

Fig. 6. OH18N9 steel. Structure after annealing: 650°C, 100 hours. $M_{23}C_6$ carbons on boundary between grains and in grains. Carbon extraction replica. Magnified 25000 x.

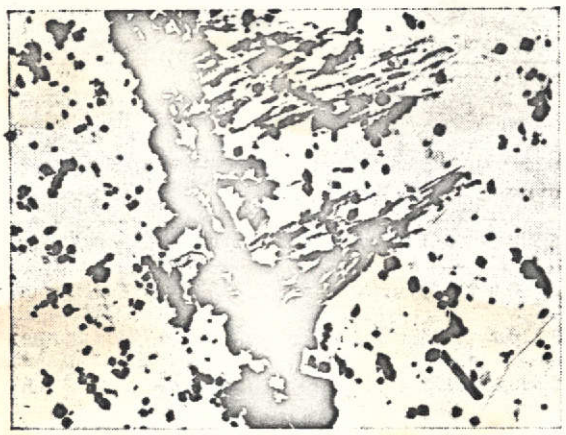

Fig. 7. OH18N9 steel. Structure after annealing: $M_{23}C_6$ carbides on boundary between grains and in grains. Strip-like growth of carbides into one grain in spots. Electron microscope. Carbon extraction replica. Magnified 15500 x.

Fig. 8. OH18N9 steel. Structure after annealing: 650°C, 1000 hours. $M_{23}C_6$ carbides on boundary between grains and in grains. Strip-like growth of carbides into both grains. Electron microscope. Carbide extraction replica. Magnified 15500 x.

Fig. 9. OH18N9 steel. Structure after annealing: 650°C, 1000 hours. $M_{23}C_6$ carbides growing out in strips from inclusion or primary precipitate in grain. Electron microscope. Carbide extraction replica. Magnified 4000 x.

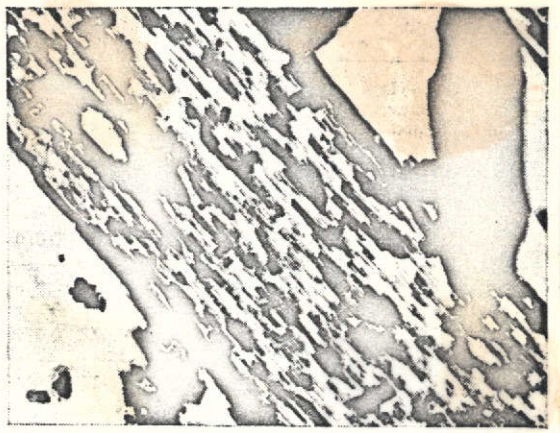

Fig. 10. Enlarged fragment of structure in Fig. 9. Magnified 25000 x.

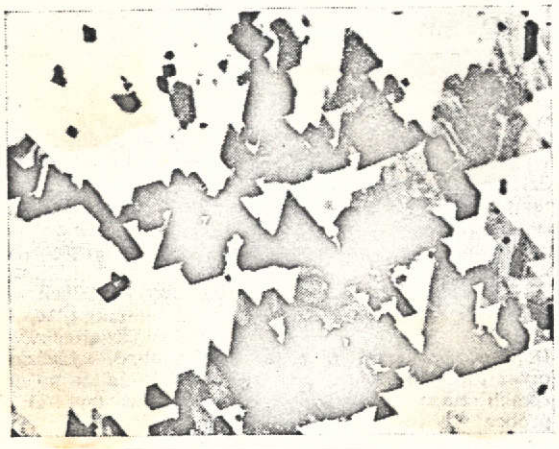

Fig. 11. OH18N9 steel. Structure after annealing: 650°C, 100 hours. $M_{23}C_6$ carbides in grains. Electron microscope. Carbide extraction replica. Magnified 25000 x.

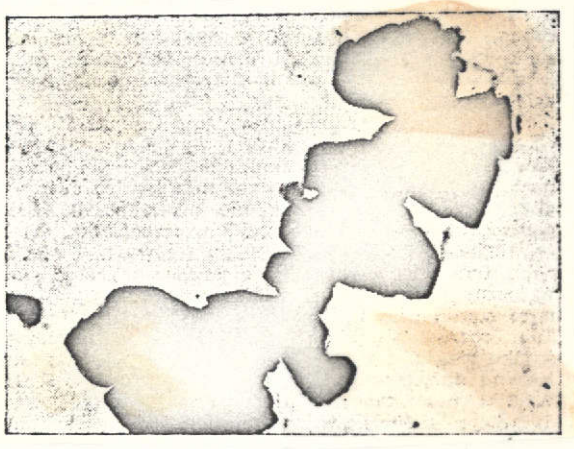

Fig. 12. OH18N9 steel. Structure after annealing: 750°C, 100 hours. Large $M_{23}C_6$ irregularly shaped carbides on boundary between grains. Electron microscope. Carbide extraction replica. Magnified 25000 x.

Table 2. Phase Composition of Precipitates in OH18N9 Steel in Relation to Temperature and Annealing Time.

Materiał wyjściowy (stan przesycony)	Warunki wyżarzania: temperatura °C	czas, h: 10	100	1000
VC—ślady	500	VC — ślady	$M_{23}C_6$ — b. mało VC — ślady	$M_{23}C_6$ — b. mało VC — ślady
	650	$M_{23}C_6$ VC — ślady	$M_{23}C_6$	$M_{23}C_6$
	750	$M_{23}C_6$	$M_{23}C_6$	$M_{23}C_6$

Key:
a--original material (solution heat treatment)
b--annealing conditions
c--temperature, °C
d--time, hours
e--traces
f--very small amount

The results of the x-ray phase analysis of segregations (Table 2) show that very small amounts of $M_{23}C_6$ carbide are precipitated already at 500°C and an annealing time exceeding 100 hours. At 650°C and 750°C only the $M_{23}C_6$ carbide is precipitated.

The hardness of the steel for all temperatures and annealing times is HV = 130-160 and its value is highest at 650°C.

4.2. IH18N10T Steel

2.1. Original structure (after solution heat treatment)

Light microscope studies of unetched metallographic specimens showed the presence of oxides and sulfides and also of two types of precipitates designated as A and B. X-ray microanalyzer studies /14 of the inclusions determined showed the presence of oxides. They also showed that inclusions of type A (Figs. 15, 16) are TiC carbides containing Fe. These precipitation strips also include other small precipitates containing Al. Precipitates of type B were not identified in this grade of steel.

Light microscope studies of etched metallographic specimens revealed a pure austenitic structure (without δ-Fe) with numerous regularly shaped precipitates and a gray coloration characteristic of M(C,N) precipitates which are rich in coal.

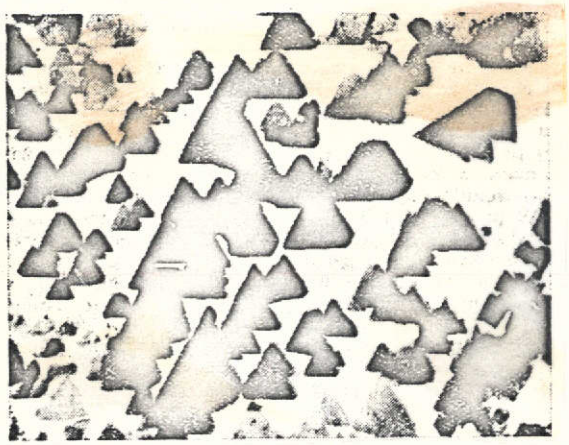

Fig. 13. OH18N9 steel. Structure after annealing: 750°C, 1000 hrs. Groups of triangular $M_{23}C_6$ carbides in grain. Electron microscope. Carbide extraction replica. Magnified 25000 x.

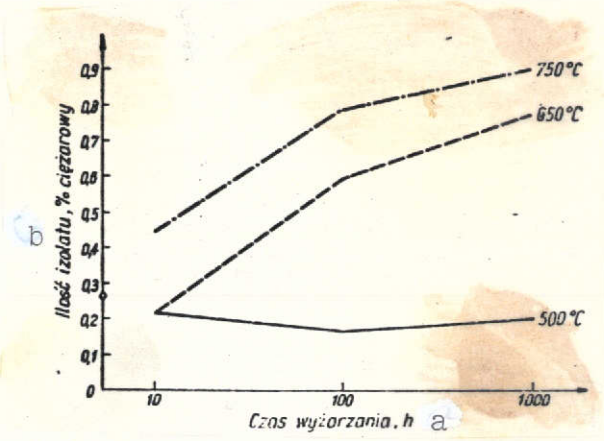

Fig. 14. OH18N9 steel. Amount of segregations vs. temperature and annealing time.
Key: a--annealing time
b--amount of segregations, weight %.

Fig. 15. IH18N10T steel. Light microscope. Magnified 500 x.

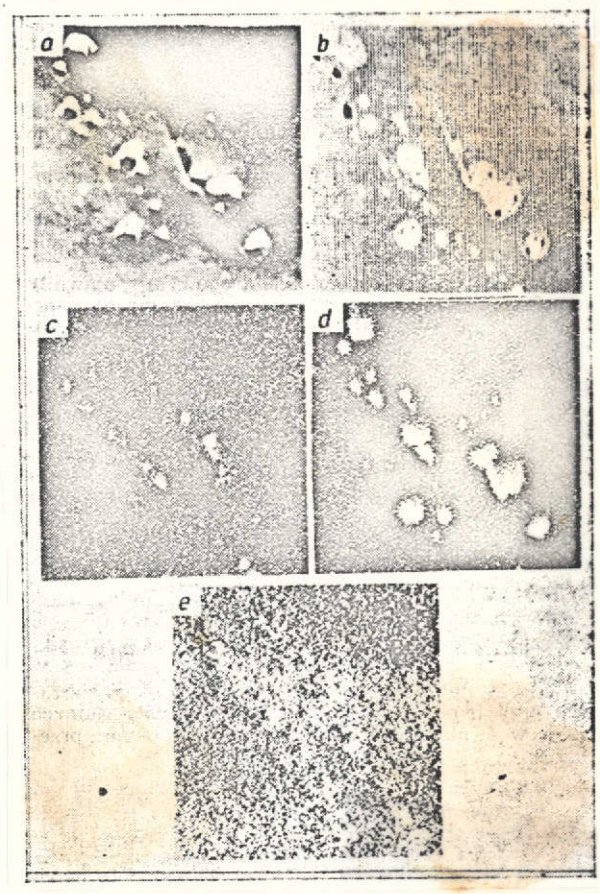

Fig. 16 ➧
Distribution of elements in precipitates in Fig. 15: a--topographic electron pattern b--electron absorption pattern. c--Al distribution. d--Ti distribution. e--Fe distribution. X-ray microanalyzer. Magnified 1200 x 0.55 [sic].

Electron microscope studies revealed an austenitic structure with weakly marked grain boundaries. Several large precipitates and many small precipitates with rounded shapes were detected in the grains (Fig. 17). Additional studies of extraction replicas taken from a metallographic specimen etched in an alcohol bromine solution detected a large number of minute precipitates having the same character. The application of electron diffraction led to crystallization of precipitates in a regular face centered system with a lattice constant corresponding to TiC..

According to the x-ray phase analysis, the segregations contained 0.54 weight % TiC, TiN and a small amount of Ti_4S_2C. The hardness of the steel was HV = 152.

4.2.2. Structure after annealing

The light microscope studies of specimens annealed at 500°C did not reveal any changes in the structure in comparison with the solution heat treated specimens. Annealing for 10 hours at 650°C causes pronounced etching of the grain boundaries, which may indicate the beginning of the precipitation process. Annealing at the same temperature for 100 and 1000 hours reveals clearly precipitates along the grain boundaries. However the boundaries themselves are more weakly etched than in a specimen annealed for 10 hours.

Annealing at 750°C for 10, 100 and 1000 hours causes smaller changes in the appearance of the structure in comparison with solution heat treatment than annealing at 650°C. The precipitates in the grains are less visible and only some boundaries are outlined clearly.

Electron microscope studies of specimens annealed at 500°C do not show the presence of the precipitation process. Chains of minute precipitates along some grain boundaries (Fig. 18) can be seen in the steel and in the solution heat treated specimen throughout the entire annealing time. These precipitates were identified by electron diffraction as TiC.

Fig. 17. IH18N10T steel. Structure after solution heat treatment. Small TiC precipitates. Electron microscope. Carbide extraction replica. Magnified 25000 x.

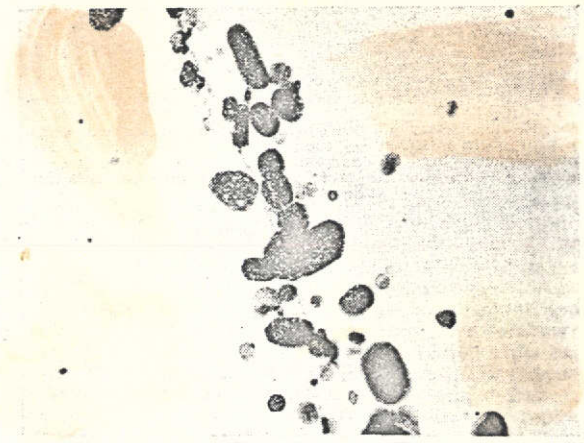

Fig. 18. IH18N10T steel. Structure after annealing: 500°C, 100 hours. Small TiC carbide precipitates along boundaries between grains. Electron microscope. Carbide extraction replica. Magnified 25000 x.

Annealing at 650°C causes the precipitation of large carbides throughout the entire annealing time, mainly along the grain boundaries. Fig. 19 shows the precipitations in a specimen annealed for 10 hours. The precipitates in specimens annealed for 100 and 1000 hours were identified as $M_{23}C_6$.

Compared to specimens annealed at 500°C, greater changes were not detected in specimens annealed at 750°C. Small carbides, mainly distributed along some grain boundaries, are visible. A new element in the structure are small needles in specimens annealed for 100 and 1000 hours. No electron diffraction patterns making identification possible were obtained from them. According to W. Koch's assumption [7] it is the σ-phase (Fig. 20). Studies of the amount of segregations (Fig. 21) do not show the presence of the precipitation process at 500°C. Annealing at 650°C causes an increase in the amount of segregations (compared to heat solution treatment) from 0.54% to about 0.8% already in the first 10 annealing hours. Prolongation of the annealing time to 1000 hours does not cause an

additional increase in the amount of segregations. Annealing at 750°C not exceeding 100 hours causes precipitation of carbides. After more than 100 hours the amount of segregations increases, however without attaining 0.8% after 1000 hours.

Fig. 19. IH18N10T steel. Structure after annealing: 650°C, 10 hours. $M_{23}C_6$ carbide network on boundaries between grains. Electron microscope. Carbide extraction replica. Magnified 4000 x.

Fig. 20. IH18N10T steel. Structure after annealing: 700°C, 100 hours. Small carbides, partially with rounded shapes. Occasional small needles (according to W. Koch [7], the σ-phase). Carbide extraction replica. Magnified 25000 x.

According to the x-ray phase analysis (Table 3) no new phases are precipitated at 500°C during the annealing. TiC, TiN and $Ti_4S_2C_2$ were detected as in the solution heat treated specimen. The presence of the $M_{23}C_6$ carbide was detected in all specimens annealed at 650°C. The $M_{23}C_6$ carbide was detected in a specimen annealed at 750°C for 10 hours. Traces of the σ-phase appear side by side with this carbide when the annealing time is longer.

The hardness of the steel for all annealing temperatures and times is HV = 155-175 and it has the highest value at the 650°C annealing temperature.

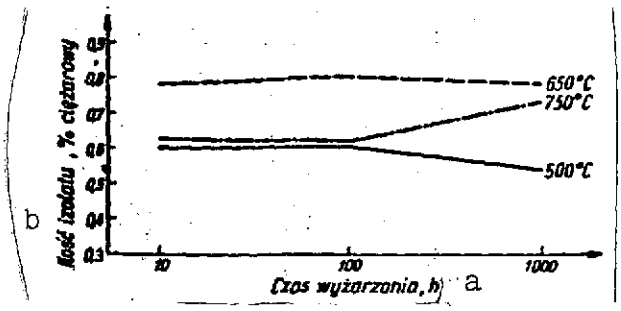

Fig. 21. IH18N10T steel. Amount of segregations vs. temperature and annealing time. Key: a--annealing time, hours
b--amount of segregations weight %

Table 3. Phase Composition of Precipitates in IH18N10T Steel in Relation to Temperature and Annealing Time.

a Materiał wyjściowy (stan przesycony)	Warunki wyżarzania b		
	c temperatura °C	d czas, h	
		10	100	1000
TiC TiN $Ti_4S_2C_2$ — mało e	500	TiC TiN $Ti_4S_2C_2$ — mało e	TiC TiN $Ti_4S_2C_2$ — mało e	TiC TiN $Ti_4S_2C_2$ — mało e
	650	TiC $M_{23}C_6$ TiN — b. mało $Ti_4S_2C_2$ — b. mało f	$M_{23}C_6$ TiC TiN — b. mało $Ti_4S_2C_2$ — b. mało f	$M_{23}C_6$ TiC TiN — b. mało $Ti_4S_2C_2$ — b. mało f
	750	TiC $M_{23}C_6$ TiN — b. mało f $Ti_4S_2C_2$ — ślady g	TiC $M_{23}C_6$ — mało e TiN — b. mało f $Ti_4S_2C_2$ — mało e o — ślady g	TiC $M_{23}C_6$ — mało e TiN — ślady g $Ti_4S_2C_2$ — ślady g o — ślady g

Key: a--original steel (solution heat treatment)
b--annealing conditions
c--temperature
d--time, hours
e--small amount
f--very small amount
g--traces

4.3. IH18N10T+B Steel

4.3.1. Original structure (after solution heat treatment)

Light microscope studies of etched metallographic specimens showed the presence of oxides, sulfides and type A precipitates. X-ray microanalyzer studies of the inclusions determined also confirmed the presence of oxides as well as the presence of calcium aluminosilicate and tetracalcium aluminoferrite relative to the potassium and iron. Inclusions of type A were identified as TiC carbides also containing iron and oxygen. In this particular steel these precipitates are accompanied by small precipitates containing aluminum. In addition, precipitates containing nitrogen, probably TiN, inclusions were detected in other areas in the metallographic specimen.

Light microscope studies of etched metallographic specimens revealed a pure austenitic structure (without δ-Fe) with numerous regularly shaped precipitates having a grey coloration, characteristic of M(C,N) specimens rich in coal, and partially a golden coloration, characteristic of M(C,N) precipitates rich in nitrogen.

The electron microscope studies revealed an austenitic structure with weakly marked grain boundaries. Large precipitates with shapes characteristic of M(C,N) carbonitrites and minute rounded TiC precipitates in smaller amounts than in IH18N10T steel were detected in the grains.

According to the x-ray phase analysis, the segregations included 0.55 weight % TiC, TiN and $Ti_4S_2C_2$. The hardness of the steel was HV = 153.

4.3.2. Structure after annealing

Light microscope studies of specimens annealed at 500°C up to 1000 hours did not reveal changes in the structure in comparison with the solution heat treated specimens. Annealing at 650°C for 10 hours causes pronounced etching of the grain boundaries, which may indicate the beginning of the precipitation process. Specimens annealed at this temperature for 100 and 1000 hours have clearly visible precipitates along the grain boundaries. Specimens annealed at 750°C have a structure which approaches that of specimens annealed at 500°C. The results of the light microscope studies described are very similar to the results obtained from the studies of IH18N10T steel.

Electron microscope studies of specimens annealed at 500°C revealed many small rounded precipitates along some grain boundaries.

Annealing at 650°C causes both the precipitation of large type $M_{23}C_6$ carbides and small, predominantly elongated carbides along the grain boundaries from which electron diffraction patterns could not be obtained (Fig. 22). These are also probably $M_{23}C_6$ carbides. The number of precipitates in specimens annealed at 750°C is smaller than in specimens annealed at 650°C, and they have predominantly /16 the character of precipitates observed in specimens annealed at 500°C (small and rounded). $M_{23}C_6$ carbides occur side by side with them, and small needle-shaped precipitates which could not be identified by electron diffraction (Fig. 23) occur in specimens annealed for more than 100 hours. It can be assumed that this is the σ phase.

Fig. 22. IH18N10T+B steel. Structure after annealing: 650°C, 100 hours. Precipitation of carbides on boundary between two grains. Electron microscope. Carbide extraction replica. Magnified 25000 x.

Fig. 23. IH18N10T+B steel. Structure after annealing: 750°C, 100 hours. Large carbide groups on boundary between two grains. Electron microscope. Carbide extraction replica. Magnified 25000 x.

Studies of the amount of segregations (Fig. 24) did not reveal the precipitation process during annealing at 500°C. Annealing at 650°C increases the amount of segregations during the first 100 hours and a prolongation of the annealing time does not cause an

additional increase in the amount of segregations. During annealing at 750°C, the precipitation occurs during the first 10 hours and prolongation of the annealing time does not cause an additional increase in the amount of segregations. At 750°C fewer segregations occur than at 650°C.

The results of the x-ray phase analysis (Table 4) show that the precipitation process does not take place at 500°C. Only TiC, TiN and $Ti_4S_2C_2$ and therefore the same phases as in solution heat treated samples were detected in the specimens studied. The $M_{23}C_6$ carbide appears in all specimens annealed at 650°C and the amounts of this carbide in specimens annealed for 100 and 1000 hours is greater than in the specimen annealed for 10 hours. The σ phase appeared in small amounts in a specimen annealed for 1000 hours at 750°C. The hardness of the steel for all temperatures and annealing times lies in the range HV = 155-167.

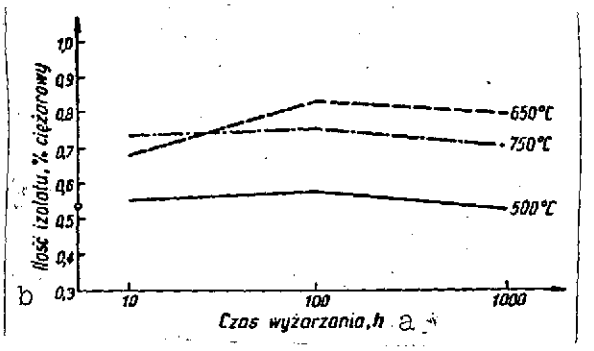

Fig. 24. IH18N10T+B steel. Amount of segregations vs. temperature and annealing time.
Key: a--annealing time, hours
b--amount of segregations in weight %

Table 4. Phase Composition of Precipitates in IH18N10T+B Steel in Relation to Temperature and Annealing Time.

a Materiał wyjściowy (stan przesycony)	b Warunki wyżarzania			
	c temperatura °C	d czas, h		
		10	100	1000
TiC TiN $Ti_4S_2C_2$	500	TiC TiN $Ti_4S_2C_2$	TiC TiN $Ti_4S_2C_2$	TiC TiN $Ti_4S_2C_2$
	650	TiC $M_{23}C_6$ TiN $Ti_4S_2C_2$	$M_{23}C_6$ TiC TiN $Ti_4S_2C_2$	$M_{23}C_6$ TiC TiN $Ti_4S_2C_2$
	750	TiC $M_{23}C_6$ TiN — e mało $Ti_4S_2C_2$	TiC $M_{23}C_6$ TiN — e mało $Ti_4S_2C_2$	TiC $M_{23}C_6$ TiN — mało e $Ti_4S_2C_2$ σ — mało e

Key: a--original steel (solution heat treatment)
b--annealing conditions
c--temperature °C
d--time, hours
e--small amount

4.4. IH18N10MT Steel

4.4.1. Original structure (after solution heat treatment)

Light microscope studies of unetched specimens showed the presence of oxides, sulfides and two types of precipitates designated as A and B (Fig. 25). The x-ray microanalyzer studies confirmed the presence of oxides. Precipitates type A were identified as TiC carbide (also containing iron) and precipitates type B as (Ti,Fe) (S,C) (Fig. 26).

Fig. 25. IH18N10MT steel. Structure after solution heat treatment. Precipitates type B. Light microscope. Magnified 500 x.

Light microscope studies of etched specimens revealed an austenitic structure with δ-Fe occurring mainly in the contact area of three austenite grains, or on the boundary between two austenite grains (Fig. 27). Gray M(C,N) precipitates rich in coal, and in smaller amounts, golden precipitates rich in nitrogen, were observed in the grains.

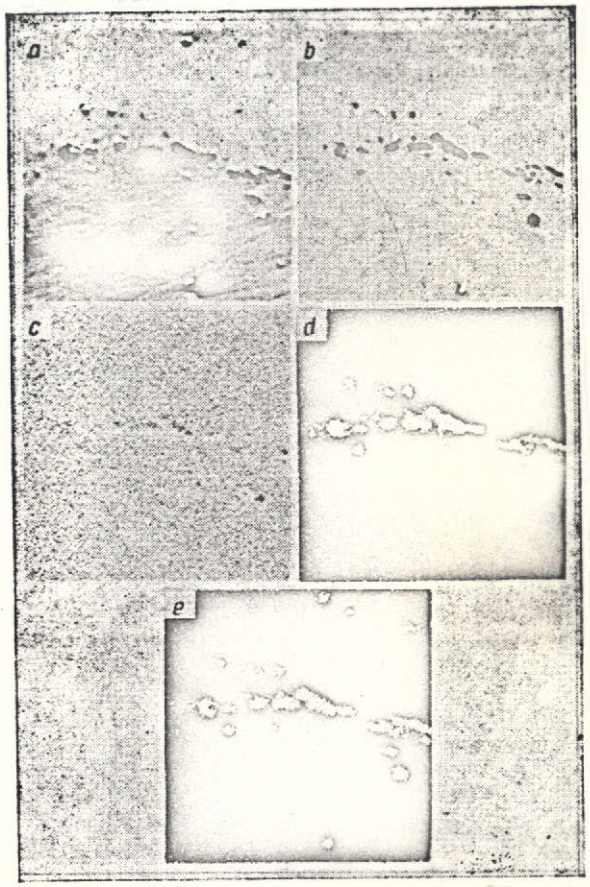

Fig. 26. Distribution of elements in precipitates in Fig. 25: a. Topographic electron image, b. electron absorption image, c. Fe distribution, d. S distribution, e. Ti distribution. x-ray microanalyzer. Magnified 1200 x 6.55 [sic].

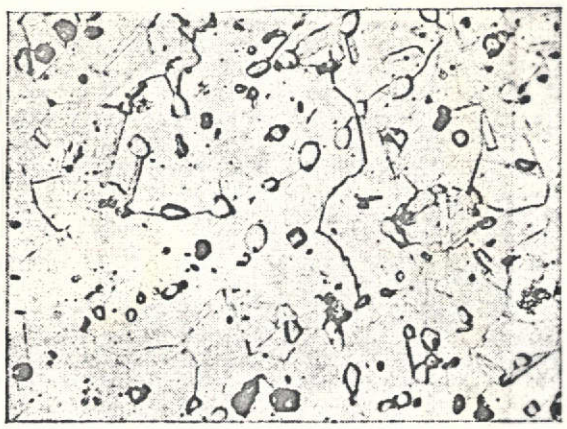

Fig. 27. IH18N10MT steel. Structure after solution heat treatment. Austenite and ferrite δ M(C, N) precipitates. Light microscope. Magnified 500 x.

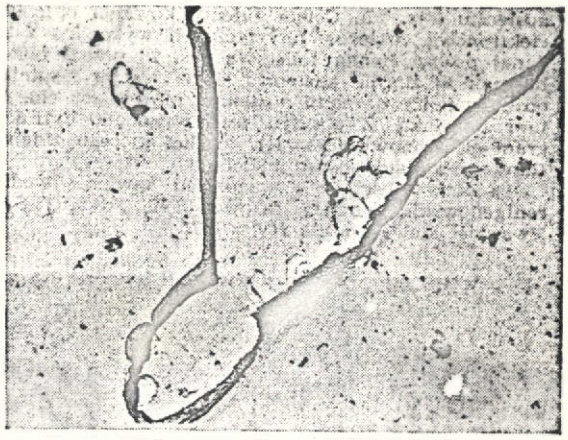

Fig. 28. Structure after solution heat treatment. Austenite and δ ferrite. Electron microscope carbide matrix replica, Cr shaded. Magnified 25,000 x.

Fig. 29. IH18N10MT. Structure after solution heat treatment. Austenite with clearly visible twin crystal. Electron microscope. Thin foil. Magnified 25,000 x.

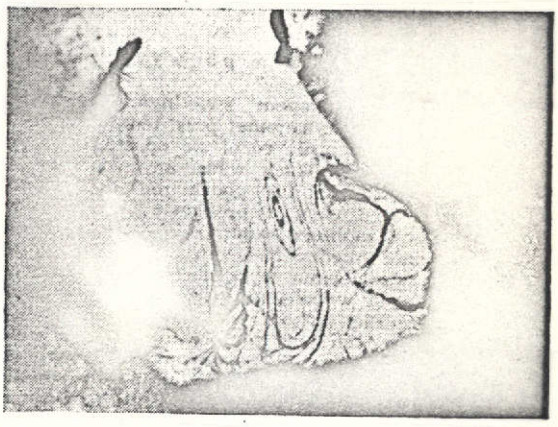

Fig. 30. IH18N10MT steel. Structure after solution heat treatment. Electron microscope. Thin foil. Magnified 25,000 x.

Electron microscope studies conducted using carbide matrix replicas detected δ ferrite zones clearly separated from the aus- /18
tenite (Fig. 28). A thin foil was made from the specimen studied in order to identify the ferritic zones by electron diffraction. Fig. 29 shows a twin crystal in an austenite grain and Fig. 30 the clearer zone between austenite grains which do not have the character of a twin crystal. On the basis of the electron diffraction pattern of this zone, the zone investigated was identified as ferrite (Fig. 31).

According to the x-ray phase analysis the segregations contained 0.6 weight % TiC, TiN, and $Ti_4S_2C_2$. The hardness of the steel was HV = 147.

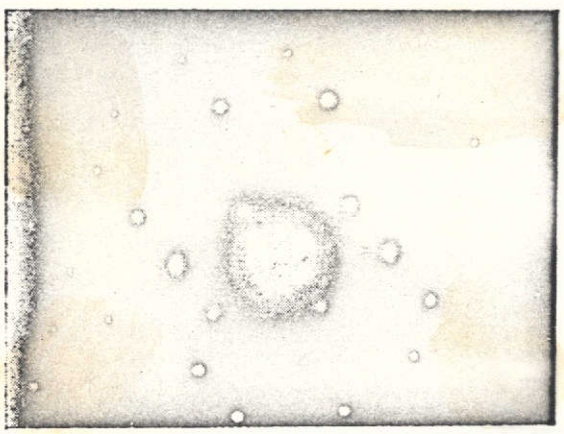

Fig. 31. Electron diffraction pattern of clearer zone in Fig. 30. Ferrite.

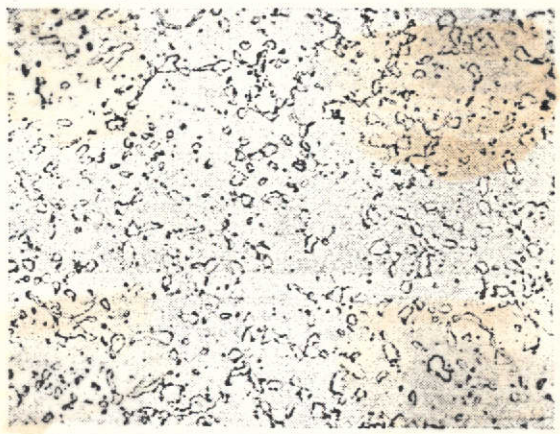

Fig. 32. IH18N10MT steel. Structure after annealing: 750°C, 1000 hours. σ phase precipitates. Light microscope. Magnified 500 x.

4.4.2. Structure after annealing

Light microscope studies have shown that the structure of a specimen annealed at 500°C for 10 hours does not differ from the structure of the solution heat treated sample. Precipitates were not detected in specimens annealed at this temperature for 100 and

1000 hours. In specimens annealed at 650°C the following can be observed: thicker boundaries between the ferrite and austenite, and after 100 hours, precipitates in ferritic zones and on the boundaries between austenite grains. Disintegration of δ ferrite and the formation of large σ phase zones can be seen in specimens annealed at 750°C. Precipitates in δ-ferrite grains can be seen in specimens annealed for 10 hours, whereas many large σ-phase zones can be seen in a specimen annealed for 1000 hours (Fig. 32). A specimen annealed for 100 hours has an intermediate structure.

Studies of this steel using the electron microscope were complicated by the reaction products formed while the replicas were taken off electrolytically from the metallographic specimen with a two-phase (austenite and ferrite) matrix which settled on the replicas. Precipitates were observed on replica zones with relatively few impurities. Small precipitates, identified as TiC were observed, mainly along the grain boundaries, in specimens annealed at 500°C. The precipitation process was not observed in a specimen annealed for 10 hours at 650°C, whereas numerous precipitates were detected in specimens annealed for 100 and 1000 hours, mainly in ferritic zones. /19

Specimens annealed at 750°C include a very large amount of precipitates with different shapes. Small rounded precipitates of the type that occurs during the solution heat treatment, minute precipitates with sharp corners and numerous σ-phase precipitates in the shape of needles can be seen (Fig. 33). A thin foil was made from a specimen annealed at 750°C for 1000 hours and it was established that zones having the shape of the δ-Fe grains (from the solution heat treated specimens) are the σ phase (Figs. 34, 35). Studies of the amount of segregations (diagram in Fig. 36) do not show the presence of the precipitation process during annealing at 500°C. At 650°C the precipitation occurs during the first 100 annealing hours; the amount of segregations does not increase with a longer annealing time. Annealing at 750°C causes sudden precipita-

tion. The amount of segregations increases with the annealing time, reaching 6.2% after 1000 hours (in the remaining steels studied it is below 1%).

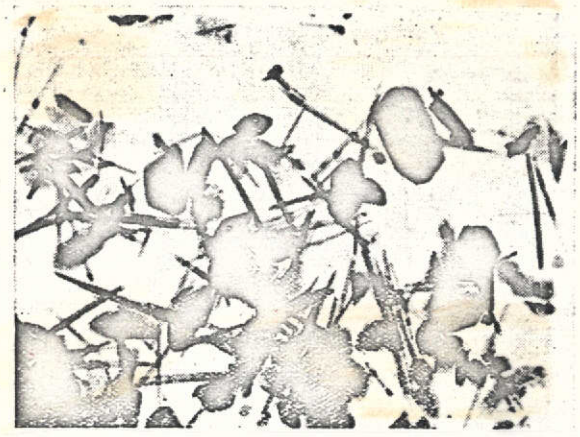

Fig. 33. IH18N10MT steel. Structure after annealing: 750°C, 1000 hours. Minute precipitates, partially with regular shapes and σ-phase needles. Electron microscope. Carbide extraction replica. Magnified 25000 x.

Fig. 34. IH18N10MT steel. Structure after annealing: 750°C 1000 hours. Austenite and zones with shape corresponding to δ-ferrite grains during solution heat treatment. Electron microscope. Thin foil. Magnified 15500 x.

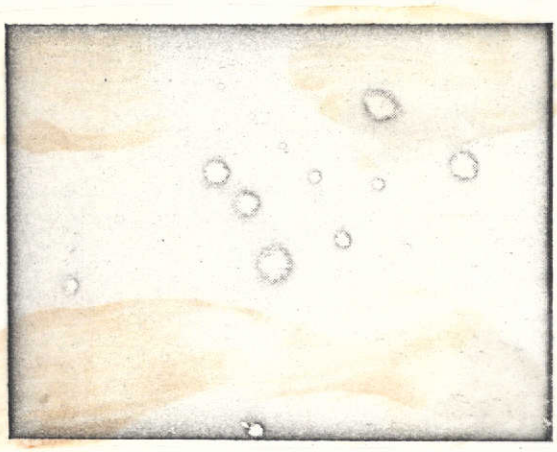

Fig. 35. Electron diffraction pattern of zone marked by arrow in Fig. 34. σ phase.

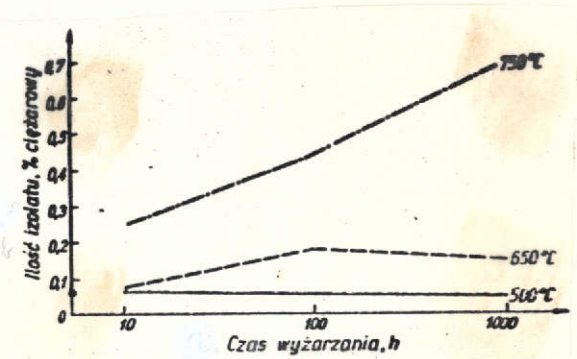

Fig. 36. IH18N10MT steel. Amount of segregations vs. temperature and annealing time. Key: a--annealing time
b--amount of segregations, weight %

Table 5. Phase Composition of Precipitates in IH18N10MT Steel in Relation to Temperature and Annealing Time.

Materiał wyjściowy (stan przesycony)	Warunki wyżarzania			
	temperatura °C	czas, h		
		10	100	1000
TiC TiN — b. mało $Ti_4S_2C_2$	500	TiC TiN — b. mało $Ti_4S_2C_2$	TiC TiN — b. mało $Ti_4S_2C_2$	TiC TiN — b. mało $Ti_4S_2C_2$
	650	TiC $Ti_4S_2C_2$ — b. mało	TiC $Ti_4S_2C_2$ — b. mało σ — mało	TiC $Ti_4S_2C_2$ — ślady σ — mało
	750	TiC — mało $M_{23}C_6$ — mało $Ti_4S_2C_2$ — ślady σ — mało	TiC — mało $M_{23}C_6$ — b. mało $Ti_4S_2C_2$ — ślady σ — mało	TiC — mało $M_{23}C_6$ — b. mało $Ti_4S_2C_2$ — ślady σ — mało

Key:
a--original steel (solution heat treatment)
b--annealing conditions
c--temperature
d--time, hours
e--very small amount
f--small amount
g--traces

The results of the x-ray phase analysis (Table 5) show that the precipitation process does not occur at 500°C. The same phases (TiC, TiN and $Ti_4S_2C_2$) occur in specimens annealed at this temperature. The σ phase was detected in specimens annealed at 650°C for 100 and 1000 hours. These phases also occur in all specimens annealed at 750°C. Minute $M_{23}C_6$ carbide amounts also occur at this temperature.

The hardness of the steel for all temperatures and annealing times lies in the range HV = 160-200.

4.5. IH18N10T"s" Steel

4.5.1. Original structure (after solution heat treatment)

The light microscope studies of unetched metallographic specimens showed the presence of oxides, sulfides and three types of precipitates designated as A (Fig. 37), B (Fig. 39) and C (Fig. 41). The x-ray microanalyzer studies confirmed the presence of oxides.

Precipitates type A are TiC carbides with a specific iron content which are accompanied by small precipitates containing aluminum (Fig. 38). Precipitates type B can be identified as (Ti,Fe)(S,C) (Fig. 40).

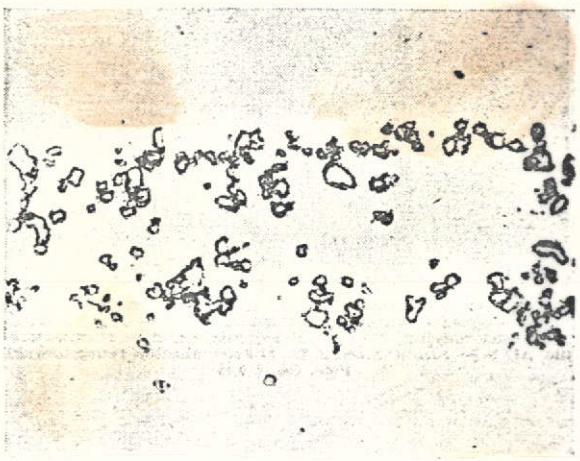

Fig. 37. IH18N1T"s" steel. Structure after solution heat treatment. Precipitates type A. Light microscope. Magnified 500 x.

Precipitates type C were too small for x-ray microanalyzer studies.

The eight microscope studies of etched metallographic specimens revealed an austenitic structure with δ-Fe strips and M(C,N) type precipitates.

Electron microscope studies detected narrow elongated δ-Fe zones along the austenite grain boundaries, few precipitates on some ferrite-austenite phase boundaries, and occasional precipitates in the ferrite and austenite. Fig. 42 shows a chain of precipitates not connected with any boundary. The small precipitates had the character of the TiC carbides identified in the steels studied earlier.

According to the x-ray phase analysis, the segregations contained 0.35 weight % TiC, TiN (a very small amount) and $Ti_4S_2C_2$. The hardness of the steel was HV = 145.

4.5.2. Structure after annealing

Light microscope studies have shown that the structure of specimens annealed at 500°C for 10 and 100 hours does not differ from the structure of a specimen subjected to solution heat treatment. /21 Susceptibility of the δ-ferrite strips to the effect of the etching agent was observed in a specimen annealed for 1000 hours. Annealing at 650°C and 750°C causes precipitation in the δ-ferrite strips. However no precipitates occur along the boundaries between the austenite grains.

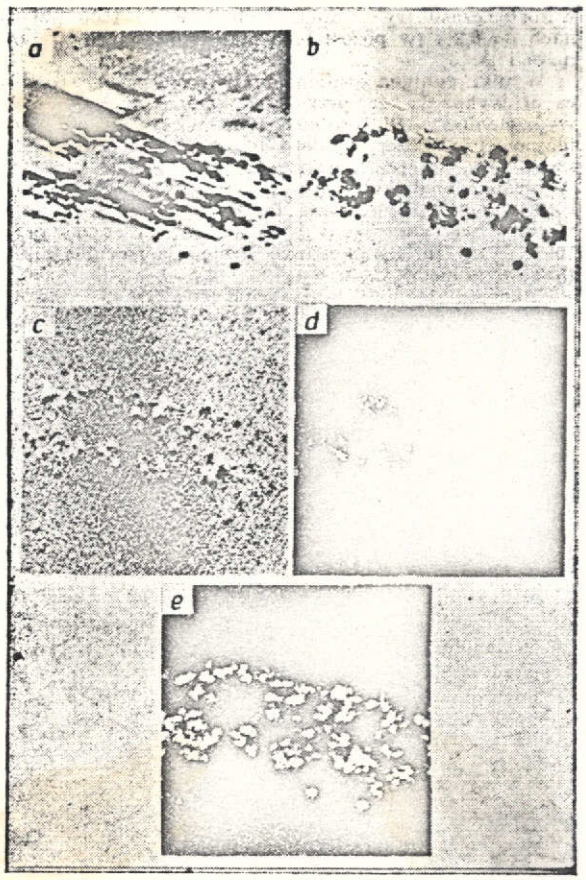

Fig. 38. Distribution of elements in precipitates from Fig. 37. a--topographic electron image. b--electron absorption image. c--Fe distribution. d--Al distribution. e--Ti distribution. X-ray microanalyzer. Magnified 600 x 0.55 [sic]

Fig. 39. IH18N10T"s" steel. Structure after solution heat treatment. Precipitates type B. Light microscope. Magnified 500 x.

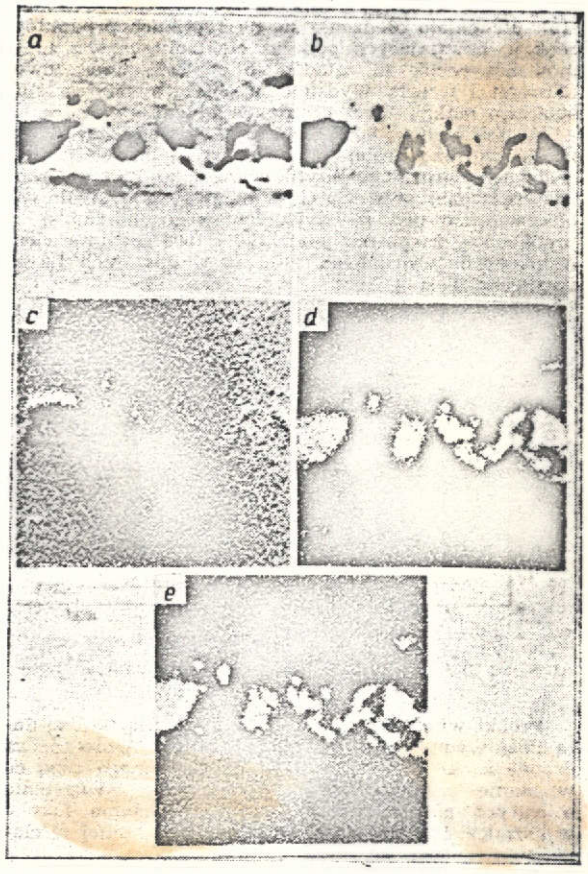

Fig. 40. Distribution of elements in precipitates from Fig. 39. (Key same as Fig. 38)

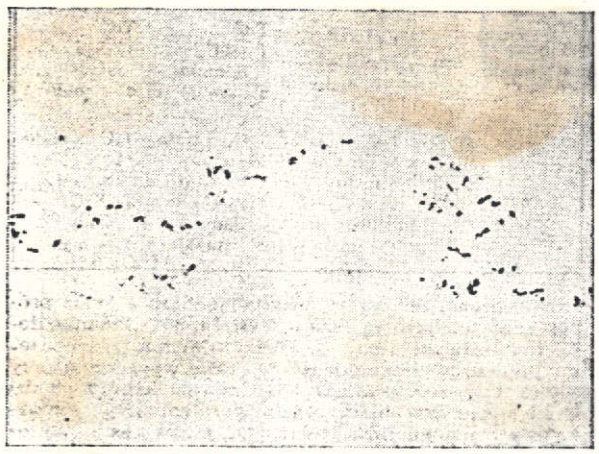

Fig. 41. IH18N10T "s" steel. Structure after solution heat treatment. Precipitates type C. Light microscope. Magnified 500 x.

Electron microscope studies of specimens annealed at 500°C have only shown the presence of few small rounded precipitates along the grain boundaries. The boundaries between the austenite and ferrite were practically free of precipitates. The studies of specimens annealed at 650°C revealed relatively few precipitates in the ferrite and few precipitates along the boundaries between the austenite grains.

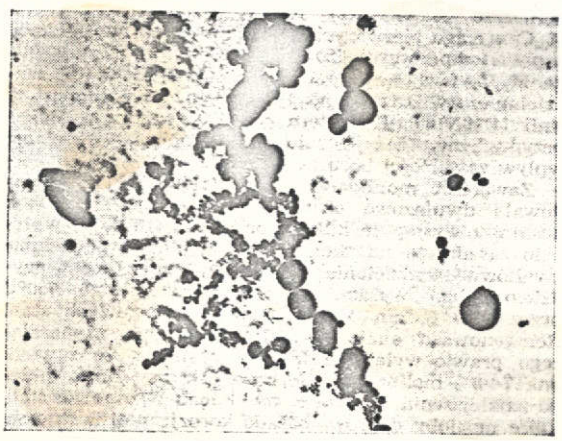

Fig. 42. Structure after solution heat treatment. Small precipitates not connected with boundary between grains. Electron microscope. Carbide extraction replica. Magnified 25000 x.

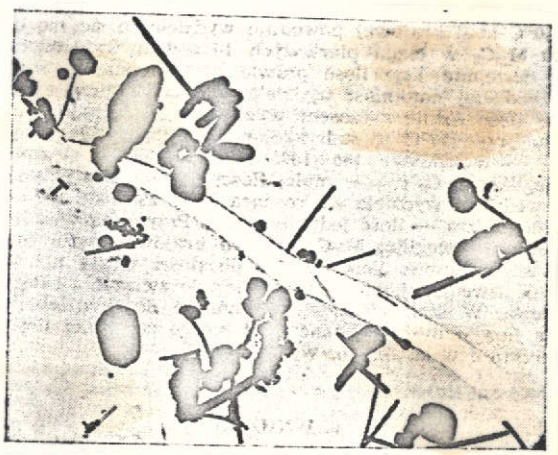

Fig. 43. IH18N10T"s" steel. Structure after annealing: 750°C, 1000 hours. Small precipitates on boundary between two rounded and needle-shaped grains. Electron microscope. Carbide extraction replica. Magnified 25000 x.

A smaller number of precipitates can be seen in specimens annealed at 750°C than in specimens annealed at 650°C. In some spots the precipitates occur along the grain boundaries in the form of small rounded precipitates (which are already visible during the solution heat treatment) and in the form of small needle-shaped σ-phase precipitates (Fig. 43). The latter occur in specimens annealed for more than 100 hours. In ferritic grains the precipitates occur relatively infrequently. Fig. 44 shows small precipitates on the boundary between the austenite and ferrite having the same shapes as those on the boundaries between the austenite grains. Large rounded precipitates occur in very few spots.

Studies of the amount of segregations (Fig. 45) did not reveal the precipitation process during annealing at 500°C. At 650°C and 750°C, annealing for 10 hours increases only slightly the amount of segregations.

Fig. 44. IH18N10T"s" steel. Structure after annealing: 750°C, 1000 hours. Precipitates on boundary between austenite and ferrite. δ-phase needles are clearly visible. Electron microscope. Carbide extraction replica. Magnified 25000 x.

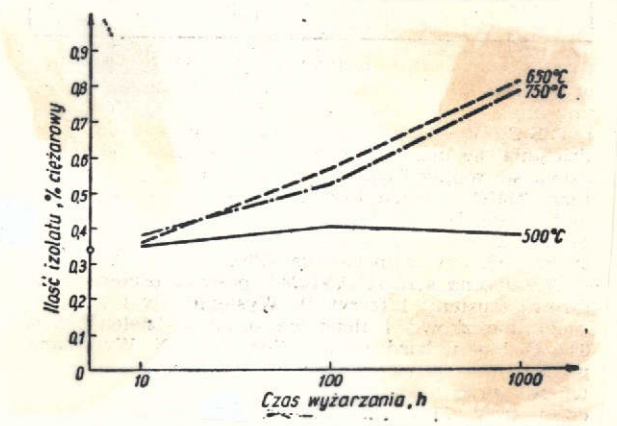

Fig. 45. IH18N10T"s" steel. Amount of segregations vs. temperature and annealing time. a--annealing time. b--amount of segregations, weight %.

The results of the x-ray phase analysis (Table 6) show that the precipitation process does not occur at 500°C. Only TiC, TiN and $Ti_4S_2C_2$ and therefore the sameephases as in the heat treated specimens were detected in the specimens studied. The σ phase (the amount of which increased with the annealing time) was detected at 650°C and 750°C after 100 and 1000 annealing hours.

5. Discussion of Results

Solution heat treated OH18N9 steel has an austenitic structure with nonmetallic inclusions (sulfides and oxides) and vanadium carbide (VC) traces. Annealing at 500°C not exceeding 10 hours does not cause precipitation of $M_{23}C_6$ carbides. After 100 and 1000 hours very small amounts of this carbide are precipitated (determined by x-ray analysis).

Solution heat treated OH18N10T steel has an austenitic structure with sulfide and oxide inclusions, TiC, TiN precipitates, and in small amounts $Ti_4S_2C_2$ precipitates. Annealing at 500°C does not cause precipitation of the phases. The $M_{23}C_6$ carbide is precipitated at 650°C. At 750°C, the $M_{23}C_6$ carbide is precipitated and after a long annealing time, the σ phase in very small amounts. The precipitation process at 750°C is less intense than at 100°C and at lower temperatures. /22

Solution heat treated IH1810T+B steel has an austenitic structure with nonmetallic sulfide and oxide inclusions, TiC, TiN and $Ti_4S_2C_2$ precipitates. Annealing at 500°C does not cause precipitation of phases. The $M_{23}C_6$ carbide is precipitated at 650°C and 750°C. A small amount of the σ phase was also detected after annealing for 1000 hours at 750°C. As in OH18N10T steel, here the precipitation process is also less intense at 750°C than at 650°C.

Solution heat treated IH18N10MT steel has ahtwo-phase (austenite and δ ferrite) matrix. Sulfide and oxide inclusions occur in

it as well as TiC, $Ti_4S_2C_2$ precipitates and a very small amount of TiN. Annealing at 500°C does not cause precipitation of phases. The σ phase is precipitated at 650°C and 750°C. The precipitation at 750°C is very intense. The $M_{23}C_6$ carbide is also precipitated during annealing at 750°C (in very small amounts compared to the precipitation of the σ phase).

Table 6. Phase Composition of Precipitates in IH18N10T"s" Steel in Relation to Temperature and Annealing Time.

a Materiał wyjściowy (stan przesycony)	b Warunki wyżarzania: c temperatura °C	d czas, h: 10	100	1000
TiC TiN — e b. mało $Ti_4S_2C_2$	500	TiC TiN — e b. mało $Ti_4S_2C_2$	TiC TiN — e b. mało $Ti_4S_2C_2$	TiC TiN — e b. mało $Ti_4S_2C_2$
	650	TiC TiN — e b. mało $Ti_4S_2C_2$	TiC σ TiN — ślady $Ti_4S_2C_2$ — mało f	T σ TiC TiN — ślady g $Ti_4S_2C_2$ — mało f
	750	TiC TiN $Ti_4S_2C_2$	TiC σ TiN — ślady g $Ti_4S_2C_2$ — mało f	σ TiC $Ti_4S_2C_2$ — mało f

Key: a--original steel (solution heat treatment)
b--annealing conditions
c--temperature
d--time, hours
e--very small amount
f--small amount
g--traces

Solution heat treated IH18N10T"s" steel has a two-phase (austenite and δ ferrite) matrix. It contains oxide and sulfide inclusions and TiC, $Ti_4S_2C_2$ precipitates and a very small amount of TiN. The small precipitates shown in Fig. 41 could not be identified. However the assumption can be made that they form one of the identified phases. Annealing at 500°C does not cause precipitation of phases. The σ phase is precipitated at 650°C and at 750°C after annealing exceeding 10 hours.

Titanium occurs in all stabilized steels in the TiC, TiN and $Ti_4S_2C_2$ precipitates which are present both in solution heat treated and annealed steels. It was established that in addition to large precipitates which are clearly visible under a light microscope, small TiC precipitates (detected under an electron microscope) exist. These are usually distributed along certain grain boundaries. Comparing the amount of segregations obtained from domestic stabilized and unstabilized steels after solution heat treatment, the assumption

can be made that they make up 0.25-0.35 weight % of the steel. In domestic stabilized steels, titanium does not completely bind the carbon, which leadss to the precipitation of the $M_{23}C_6$ carbide during the annealing of these steels.

Annealing of stabilized steels at 500°C does not cause precipitation of phases. In unstabilized steel annealed at the same temperature for more than 1000 hours, the $M_{23}C_6$ carbide is precipitated in a very small amount.

A significant effect of boron on the precipitation process was not detected. The phases are not precipitated at 500°C both in IH18N10T and IH18N10T+B steel. The $M_{23}C_6$ carbide is precipitated at 650°C during the first 10 annealing hours. At 750°C, in addition to the $M_{23}C_6$ carbide, the σ phase is precipitated. In IH18N10T steel the precipitation was detected after 100 hours whereas in IH17N10T+B steel it was detected only after 1000 hours. The assumption can be made that this is due to the effect of the boron content delaying the precipitation.

The molybdenum content in IH18N10MT steel caused a two-phase structure after solution heat treatment. Several percent of δ ferrite occurred among with the austenite, which had a fundamental effect on the precipitation process, causing a sudden precipitation of the σ phase. The amount of σ phase precipitated after annealing for more than 1000 hours at 750°C is 6 weight % of the steel. Spectral x-ray analysis of the segregations, containing almost exclusively the σ phase has shown that it contains 7-8% molybdenum. However it does not reduce the molybdenum content in the steel matrix by an amount which could lead to corrosion of the steel in sulphuric acid.

Comparing the Swedish IH18N10T"s" and the domestic IH18N10T steel, the different properties of the precipitation process should

be noted. Annealing of domestic steel at 650°C causes the precipitation of the $M_{23}C_6$ carbide during the first 10 annealing hours, after which its amount does not increase for all practical purposes. On the other hand, in the Swedish steel the σ phase is precipitated and its amount increases with the annealing time. In domestic st steel, mainly the $M_{23}C_6$ carbide is precipitated at 750°C. Its amount increases in the interval 100-1000 hours and the σ phase increases by a small amount. Only the σ phase is precipitated in the Swedish steel. Its amount increases in the interval 100-1000 hours. The reason for the precipitation of the $M_{23}C_6$ carbide in the domestic steel may be the smaller ratio of the amount of titanium to the amount of carbon than in the Swedish steel, which is insufficient to bind the entire carbon. In the Swedish steel, the tendency toward the precipitation of the σ phase may also be due to a certain amount of the δ ferrite in the original structure.

6. Conclusions

The following conclusions can be made on the basis of the studies made:

1. In the majority of steels studied titanium does not bind completely the carbon contained in them. In addition to the titanium content which is four times higher than the carbon content, $M_{23}C_6$ carbides are also precipitated during the annealing.

2. Boron does not have a pronounced effect on the precipitation process. Only a delay in the precipitation of the σ phase was detected in steel to which boron was added.

3. Molybdenum has a significant effect on the structure after solution heat treatment (δ ferrite occurs in addition to austenite) and on the precipitation process during annealing, causing the precipitation of large amounts of the σ phase, particularly during annealing at 750°C.

4. The different properties of the precipitation process in the domestic and Swedish IH18N10T steel may be caused by the higher Ti/C ratio in the Swedish steel and the presence of a certain

amount of δ ferrite in this steel after the heat solution treatment.

5. In steels containing titanium, the $Ti_4S_2C_2$ phase occurs in addition to the oxide and sulfide inclusions.

References

1. Z. Bojarski et al., Sprawodzanie Institutu Metalurgii Zelaza nr. 1185, 1965. Niepublikowane. [Unpublished Report No. 1185, Institute of Ferrous Metallurgy (1965)]

2. C. G. Nestler, Einführung in die Electronenmetallographie [Introduction to electron metallography], Oxford, 1966.

3. J. S. Brammar and M.A.P. Dewey, Specimen preparation for electron metallography, Oxford, 1966.

4. W. Bollmann, Electron Microscopy. Proceedings of the Stockholm Conference, Stockholm 1957, p. 316-319.

5. A. Rozwadowska, M. Smolinska and J. Eysymontt, Sprawozdanie Instytutu Metalurgii Zelaza nr. 1390, 1967. Niepublikowane [Unpublished Report No. 1390, Institute of Ferrous Metallurgy (1967)].

6. Z. Bojarski and J. Eysymontt, Arch. Hutn. 14, (2279(1969).

7. W. Koch, Metallkundliche Analyze [Metallographic Analysis], Dusseldorf, 1965.